pressed at the surface in a series of north-northeast prominent normal faults, including the Deep Spring fault, the fault bounding the narrow valley east of the Saline Range, and the fault west of the Cottonwood Mountains (Fig. 1). Within the Saline Range, the deformation is distributed over several smaller faults connecting with Saline Valley across late Cenozoic volcanic deposits. The morphology of these faults, both in the field and on satellite imagery, as well as geodetic measurements suggest recent activity [W. A. Bryant, *Calif. Geol.* **42** (1989); M. Rehis, in *Crustal Evolution of the Great Basin and Sierra Nevada, Field Trip Guide*, M. Lahren, J. Trexler, C. Spinisa, Eds. (University of Nevada, Reno, 1993); J. B. Minster and T. H. Jordan, *J. Geophys. Res.* **92**, 4798 (1987); T. H. Dixon, S. Robaudo, J. Lee, *Tectonics*, in press].

6. In the week after the earthquake, a portable seismic network was deployed in the Eureka Valley by seismologists from the University of Reno, Reno, NV [A. M. Asad, J. N. Louie, S. K. Pullammanappallil, *Eos* **74**, 425 (1994)].
7. The ground ruptures were observed along the base of two west-facing scarps emanating from the Saline Range and extended northward into the valley over a distance of 3 to 4 km. They consisted of left-stepping echelons, generally open fissures, some of them showing a vertical separation of 5 to 20 mm, west side down, which is consistent with the cumulative displacement expressed in the scarps' topography (S. Hecker, personal communication).
8. ERS-1 SAR data were acquired on 14 September 1992, 23 November 1992, and 8 November 1993. Raw SAR data were processed directly to interferograms (*10*).
9. A. G. Gabriel, R. M. Goldstein, H. A. Zebker, *J. Geophys. Res.* **94**, 9183 (1989).
10. In each SAR image pixel, the phase value represents a measure modulo-2π of the distance between the radar antenna and the ground. An interferogram is obtained by averaging the product of one complex SAR image and the complex conjugate of another image, after subpixel coregistration (*3*). The phase of each pixel in an interferogram is the difference of the phase of the corresponding pixels in the two SAR images.
11. The interferometric baseline is the distance between the two orbits from which the data were acquired. In an interferogram, the ambiguity height is defined as the topographic elevation difference that would produce a phase variation of 2π and is inversely proportional to the component of the baseline that is perpendicular to the satellite line of sight. In the coseismic interferogram, the ambiguity height is about 78 m and varies by 7% across the scene. On the other hand, the line-of-sight surface displacement that would produce a phase variation of 2π is 28 mm (half the radar wavelength), independent of the imaging geometry. Therefore, the sensitivity to surface displacement is about 2785 times greater than to elevation variations.
12. Differencing the phase of two interferograms requires one phase field to be scaled to the same fringe rate as the other (*3*), so at least one phase field must be unwrapped [R. M. Goldstein, H. A. Zebker, C.L. Werner, *Radio Sci.* **23**, 713 (1988)]. The ability to unwrap the phase depends on the noise level in the system and the fringe rates in the image. Because the coseismic interferogram in Fig. 2, center, has a smaller fringe rate than that in Fig. 2, left, we unwrapped the coseismic phase, scaled it to the intrinsic fringe rate of the preseismic interferogram, and computed their difference. We then unwrapped the resulting interferogram, which has many fewer fringes, and scaled the phase back to the coseismic rate (Fig. 2, right).
13. For ERS-1, the satellite line of sight is nearly perpendicular to the orbit and has an incidence angle of 23° in the center of the scene [European Space Agency, *ERS-1 System* (ESA Publications Division, ESTEC, Noordwijk, Netherlands, 1992)].
14. Atmospheric phase propagation delays estimated for L-band microwaves by the Global Positioning System can reach about 2 m through the ionospheric and tropospheric layers [D. M. Tralli and S. M. Lichten, *Bull. Geod.* **64**, 127 (1990)]. SAR interferograms probably depict variations of this signal across a scene, but the distinction from effects due to other sources is unclear.
15. In the middle of the depression, the displacement of the ground is essentially vertical, so its magnitude is given by the observed value of the range displacement divided by the cosine of the incidence angle (*13*).
16. A phase offset of 2.8 cm could arise from a phase-unwrapping error, which is most likely to occur in regions of sharp topography such as that of the Saline Range. However, when following a close contour, a phase-unwrapping error must be balanced by a phase offset of opposite sign. The fact that it is possible to connect both ends of profile CC′, following a smooth phase contour running around the zone of phase discontinuity, allows us to rule out this hypothesis.
17. Y. Okada, *Bull. Seismol. Soc. Am.* **75**, 1135 (1985).
18. The aftershock sequence includes four events of $M > 4.5$ (Fig. 1). One of them occurred near the northeast part of the subsidence basin and has the following parameters: strike = −179.3°, dip = 74° to the west, rake = −101°, depth = 5 km, and moment = 1.23×10^{16} Nm (*19*).
19. H. K. Thio and H. Kanamori, *Bull. Seismol. Soc. Am.*, in press.
20. We thank S. Hecker for providing an unpublished surface rupture map, J. Louie for providing relocated aftershock coordinates, R. Armijo for participation in field work, and E. Ivins and K. Hudnut for critically reading the first version of the manuscript. ERS-1 data were provided by the European Space Agency. The work was done at the Jet Propulsion Laboratory, California Institute of Technology, under contract with NASA.

9 December 1994; accepted 8 February 1995

Inactivation of the Type II TGF-β Receptor in Colon Cancer Cells with Microsatellite Instability

Sanford Markowitz,* Jing Wang,† Lois Myeroff,† Ramon Parsons,† LuZhe Sun, James Lutterbaugh, Robert S. Fan, Elizabeth Zborowska, Kenneth W. Kinzler, Bert Vogelstein, Michael Brattain, James K. V. Willson

Transforming growth factor–β (TGF-β) is a potent inhibitor of epithelial cell growth. Human colon cancer cell lines with high rates of microsatellite instability were found to harbor mutations in the type II TGF-β receptor (RII) gene. Eight such examples, due to three different mutations, were identified. The mutations were clustered within small repeated sequences in the RII gene, were accompanied by the absence of cell surface RII receptors, and were usually associated with small amounts of RII transcript. RII mutation, by inducing the escape of cells from TGF-β–mediated growth control, links DNA repair defects with a specific pathway of tumor progression.

TGF-β inhibits the growth of multiple epithelial cell types, and loss of this negative regulation is thought to contribute to tumor development (*1–5*). Studies have shown that TGF-β suppresses the growth of certain cancer cell lines, that antisense inhibition of TGF-β enhances the tumorigenicity of weakly tumorigenic cancer cell lines, and that certain tumor cells can become unresponsive to TGF-β (*2–5*). The TGF-β growth inhibitory signal is transduced through two receptors, type I (RI) and type II (RII), which function as a heteromeric complex (*6, 7*). We investigated whether inactivation of TGF-β receptors is a mechanism by which human colon cancer cells lose responsiveness to TGF-β. We found that RII receptors were inactivated in a subset of colon cancer cell lines. RII inactivation was common in tumor cells exhibiting microsatellite instability (hereafter referred to as RER^+, for "replication errors"), but not in RER^- cells (*8*).

We initially examined the expression of RI and RII transcripts in 38 human colon tumor cell lines using a ribonuclease (RNase) protection assay. RI transcripts were detected in all samples, whereas RII transcripts were undetectable or present at markedly reduced amounts in 12 (32%) of the samples (Fig. 1, A and B). For unrelated purposes, we had independently assayed these cell lines for the RER phenotype. Nine of 11 RER^+ but only 3 of 27 RER^- cell lines showed reduced RII expression (Fig. 1B) (*9–11*). This correlation was highly significant [probability (P) <0.001 by χ^2 test]. Southern (DNA) blot analysis indicated that loss of the RII transcript in the RER^+ cells was unlikely to be due to deletions or rearrangements of the RII gene (*12*).

To show that RII inactivation in the RER^+ cells was not simply a trait selected for during cell culture, we examined RII expression in tumor xenografts that had been de-

S. Markowitz, L. Myeroff, J. Lutterbaugh, E. Zborowska, J. K. V. Willson, Department of Medicine and Ireland Cancer Center, University Hospitals of Cleveland and Case Western Reserve University, Room 200, 11001 Cedar Road, Cleveland, OH 44106, USA.
J. Wang, L.-Z. Sun, R. S. Fan, M. Brattain, Department of Biochemistry and Molecular Biology, Medical College of Ohio, Toledo, OH 43699, USA.
R. Parsons and K. W. Kinzler, Johns Hopkins University Oncology Center, 424 North Bond Street, Baltimore, MD 21231, USA.
B. Vogelstein, Howard Hughes Medical Institute, 4000 Jones Bridge Road, Chevy Chase, MD 20815, USA, and Johns Hopkins University Oncology Center, 424 North Bond Street, Baltimore, MD 21231, USA.

*To whom correspondence should be addressed.
†These authors contributed equally to this work.

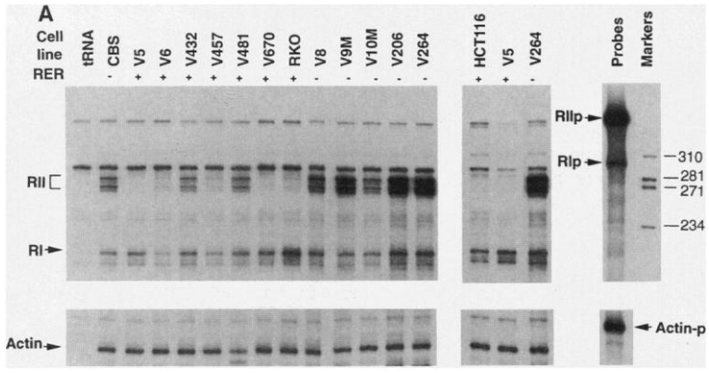

Fig. 1. (**A**) Expression of RI and RII transcripts in RER$^+$ and RER$^-$ human colon cancer cell lines. Expression of RI and RII was examined by an RNase protection assay (*14*). Total RNA (40 μg) from each sample was hybridized overnight in a single reaction to probe for RI, RII, and human γ-actin. Shown is the autoradiogram of a 7M urea–6% acrylamide gel displaying the reaction products. The RII probe (RIIp) protects a tight doublet of approximately 274 base pairs, and the RI probe (RIp) protects a 222–base pair fragment. The control γ-actin probe (Actin-p) protected a 126-bp fragment. The colon cancer cell lines are indicated above the lanes, with the VACO group of cell lines indicated by the prefix V. A control reaction displays the protection pattern generated by yeast tRNA. The two panels show results from two independent experiments. The sizes of the molecular markers are given in base pairs. (**B**) Quantitation of RII and RI transcript expression in 38 human colon cancer cell lines. RNase protection patterns [as in (A)] were quantitated by laser densitometry. The relative transcript expression in arbitrary optical density units is indicated for 11 RER$^+$ and 27 RER$^-$ cell lines. Variations in sample loading were corrected by normalizing samples for their relative expression of human γ-actin. Arrows show the mean level of receptor expression for RER$^+$ (filled arrow) and RER$^-$ cells (open arrow). The broken line indicates the limit at which the naked eye detects a protected transcript at maximally sensitive exposures.

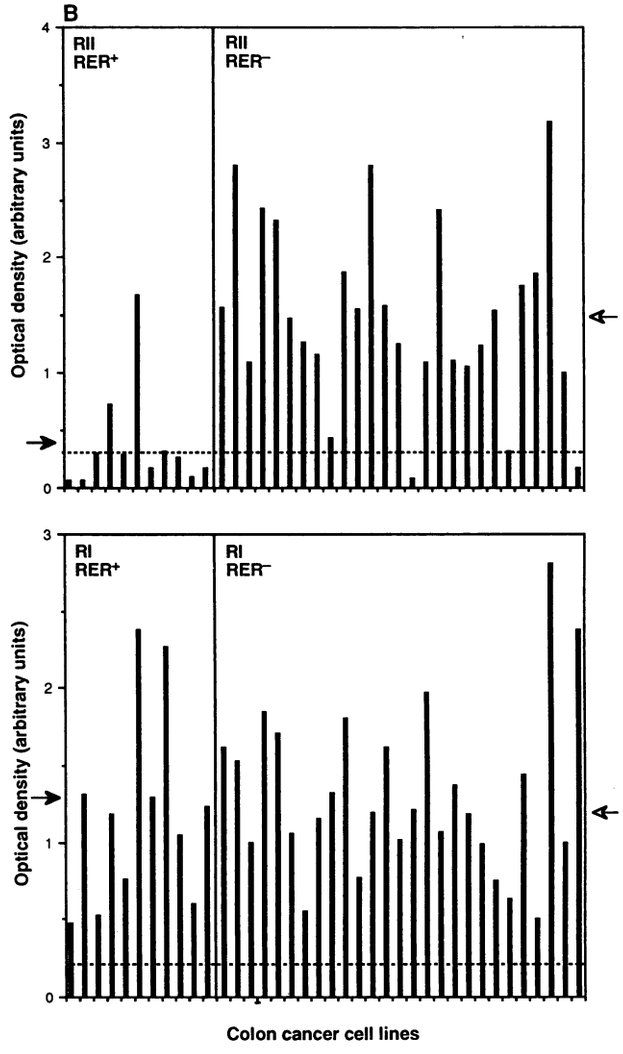

rived from 30 human colon cancers by implantation into athymic mice (*13*). RII transcripts were abundant in 25 of 27 RER$^-$ xenografts but absent in three of three RER$^+$ xenografts (Fig. 2). These three RER$^+$ xenografts were established from the same tumors as were three RER$^+$ immortalized cell lines, which also lacked RII transcript expression (Fig. 2). Loss of RII transcript was thus not an artifact of in vitro culture of the RER$^+$ cell lines.

To assay for the expression of cell surface TGF-β receptors, we performed cross-linking experiments with ^{125}I-labeled TGF-β (*14*, *15*). There was no detectable ^{125}I–TGF-β binding to any of eight RER$^+$ cell lines with reduced amounts of RII transcript (Fig. 3). The absence of RI surface receptors in these lines (Fig. 3) is consistent with previous reports that RII receptor is required for TGF-β binding to RI (*7*, *14*). A third TGF-β receptor (RIII) is expressed in most RER$^+$ and RER$^-$ cell lines (Fig. 3), but it is likely without physiologic consequence, as it is thought to function only in the presentation of ligand to RI and RII (*16*).

The RI and RII cell surface receptors were also undetectable in VACO481 cells, one of the two RER$^+$ cell lines with normal amounts of RI and RII transcripts. Although mutations in RII abolish TGF-β binding to both RI and RII, mutations in RI apparently do not affect TGF-β binding to RII (*7*, *17*). Thus, the absence of both RI and RII cell surface receptors from VACO481 cells is most easily explained by an RII mutation. A presumptive mutation was identified in an assay of RII protein synthesized in vitro (*18*) and then confirmed by sequence analysis of the complete VACO481 RII complementary DNA (cDNA). This analysis revealed a GT insertion into a six–base pair (bp) GT-GTGT repeat at nucleotides 1931 to 1936 (Fig. 4) and the absence of any normal sequence (*18*). The resulting frameshift was predicted to substitute a highly basic, 29–amino acid COOH-terminus for the

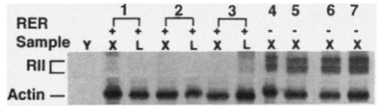

Fig. 2. RII transcript expression in colon cancer xenografts. RNase protection assays were used to measure expression of RII and γ-actin transcripts in xenografts (labeled X) established from seven different human colon tumors. Lanes labeled L contain samples from immortal cell lines established from the same tumors as the xenografts and are shown for comparison of RII expression. A control reaction displays the protection pattern generated by yeast tRNA (labeled Y).

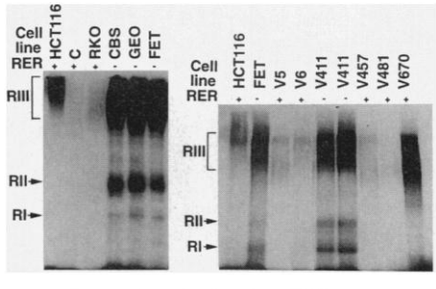

Fig. 3. Expression of cell surface TGF-β receptors in RER$^+$ and RER$^-$ human colon cancer cell lines (*14*). The VACO group of colon cancer cell lines are indicated by the prefix V. The two panels show results of two independent experiments.

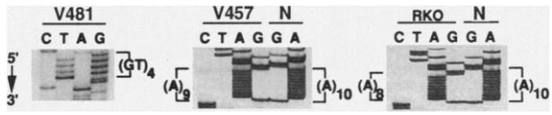

Fig. 4. Mutant RII sequences in RER+ tumor cell lines. Mutant sequences shown are for cell lines VACO481, which has a GT insertion at wild-type nucleotides 1931 to 1936, and VACO457 and RKO, in which one or two bases, respectively, have been deleted at wild-type nucleotides 709 to 718. VACO cell lines are designated by the prefix V. The normal polyadenine sequence (nucleotides 709 to 718) is displayed in the lanes labeled N. Sequencing reactions were primed on the antisense strand; therefore, juxtaposed sequences are in register relative to their 3′ ends. Sequences shown are those of the directly sequenced PCR-amplified products (VACO481, VACO457) or of a representative mutant clone of the PCR-amplified RII cDNA (RKO).

slightly acidic 33–amino acid wild-type COOH-terminus (*19*). The same RII frameshift mutation was also detected in the primary colon tumor from which the VACO481 cell line was established, but not in normal colon tissue from the same patient, indicating that the mutation was somatic and that it occurred before cell culture.

Frameshift mutations located in the 5′ half of mRNA transcripts have been associated with decreased mRNA stability (*20*). To search for this type of mutation, we sequenced the 5′ half of the RII cDNA from seven additional RER+ cell lines in which RII transcripts, though markedly reduced, could be recovered by reverse transcriptase–polymerase chain reaction (RT-PCR). In each of these cell lines an RII frameshift mutation was found (Fig. 4) (*12*). The mutations appeared homozygous (no wild-type 5′ sequences were detected) in four cell lines, and heterozygous in the three others. The mutations were all located within a sequence of 10 repeating adenines (nucleotides 709 to 718), which was truncated by either one base (four cell lines) or two bases (three cell lines) (Fig. 4). The RII genes with these one- and two-base deletions were predicted to encode truncated receptors of 161 amino acids and 129 amino acids, respectively. For three of these seven RER+ cell lines studied, there were primary colon tumors or tumor xenografts available. In each case, the same RII mutation present in the cell line was also present in the tumor sample. In two cases normal colon tissue was also available and was shown not to harbor an RII mutation.

In contrast to the RER+ colon cell lines, only a minority of RER− cell lines showed inactivation of TGF-β receptors. The RER− cell lines had RI and RII transcripts in 90% (24 of 27) (Fig. 1), RI and RII cell surface receptors in 86% (6 of 7) (Fig. 2), and growth inhibition by TGF-β in 100% (5 of 5) of the samples studied (*4*, *12*).

The RER+ samples (cell lines and xenografts) in this study were derived from predominantly right-sided (eight of nine evaluable), often metastatic (five of nine evaluable) colon cancers. However, the RER− samples also included 17 right-sided colon cancers (none with RII loss) and 32 metastatic colon cancers (only two with RII loss). Thus, loss of RII was characteristic of a cancer's RER phenotype rather than its site of origin or clinical stage. Included among our RER+ samples were two cell lines established from familial colon cancers (hereditary nonpolyposis colorectal cancer), six cell lines derived from sporadic colon cancers (*8*), five cell lines bearing mutations in a known mismatch repair gene, and four cell lines bearing only wild-type versions of these genes (*10*, *21*). The type II TGF-β receptor was thus a target for inactivation in each of the currently identified subsets of RER+ colon cancers (*8*, *10*, *21*).

Deletions and insertions in simple repeated sequences occur throughout the genome of RER+ tumors (*8*). However, inactivation of RII is likely to be a critical step in tumor progression rather than a simple correlate of the RER+ phenotype. TGF-β is expressed by normal colon epithelium (*22*), by malignant colon epithelium (*22*), and by most colon cancer cell lines (*23*). It also abolishes the in vitro proliferation of early colon neoplasms (*2*, *12*). Concordantly, RII inactivation induces escape from TGF-β–mediated growth inhibition in several cell types (*5*, *7*, *17*). Moreover, restoration of wild-type RII expression by gene transfection suppresses the in vivo tumorigenicity of receptor-negative breast and colon cancer cell lines (*12*, *14*). RII inactivation should thus directly confer a growth advantage on RER+ tumors.

Mutations in the type II TGF-β receptor thus link DNA repair defects with a demonstrable pathophysiologic event. We hypothesize that small repeat sequences in the RII gene make it a favorable target for RER+-associated mutator mechanisms. Once generated, the proliferative advantage of cells with inactivated RII would drive colon tumor progression. This pathway may also be operative in other human malignancies in which the RER+ phenotype has been detected [reviewed in (*24*)].

REFERENCES AND NOTES

1. A. Roberts and M. Spom, in *Peptide Growth Factors and Their Receptors. Handbook of Experimental Pharmacology,* A. Roberts and M. Sporn, Eds. (Springer-Verlag, Heidelberg, 1990), pp. 419–472; J. Massagué, *Annu. Rev. Cell Biol.* **6**, 597 (1990); H. Moses, E. Yang, J. Pietenpol, *Cell* **63**, 247 (1990); J. Filmus and R. Kerbel, *Curr. Opin. Oncol.* **5**, 123 (1993).
2. S. Markowitz *et al.*, *J. Clin. Invest.* **93**, 1005 (1994).
3. S. Wu *et al.*, *J. Cell. Biol.* **116**, 187 (1992); S. Wu *et al.*, *Cell Growth Differ.* **4**, 115 (1993); J. Park *et al.*, *Proc. Natl. Acad. Sci. U.S.A.* **91**, 8772 (1994); A. Manning, A. Williams, S. Game, C. Paraskeva, *Oncogene* **6**, 1471 (1991).
4. N. Hoosein *et al.*, *Exp. Cell Res.* **181**, 442 (1989).
5. A. Geiser, J. Burmester, R. Webbink, A. Roberts, M. Sporn, *J. Biol. Chem.* **267**, 2588 (1992).
6. H. Lin *et al.*, *Cell* **68**, 775 (1992); A. Moustakas *et al.*, *J. Biol. Chem.* **268**, 22215 (1993).
7. J. Wrana *et al.*, *Cell* **71**, 1003 (1992).
8. Y. Ionov *et al.*, *Nature* **363**, 558 (1993); S. Thibodeau *et al.*, *Science* **260**, 816 (1993); L. Aaltonen *et al.*, *ibid.*, p. 812; H. Kim *et al.*, *Am. J. Pathol.* **145**, 148 (1994); J. Chen *et al.*, *Cancer Res.* **55**, 174 (1995).
9. J. Eshleman *et al.*, *Oncogene* **10**, 33 (1995).
10. B. Liu *et al.*, *Nature Genet.* **9**, 48 (1995).
11. The RER+ colon cancers studied were RKO, HCT116, C, VACO432, VACO444, VACO457, VACO481, VACO5, VACO6, VACO670, and VACO703. The RER status of these lines was determined as described in (*10*).
12. S. Markowitz *et al.*, unpublished data.
13. Human colon cancer tissue (5 mm^2), obtained at surgical resection, was subcutaneously implanted into the forelimbs of athymic mice. Xenografts were removed when they were 1000 mm^3 in size. All animal procedures were in accordance with guidelines of the institutional animal care committee.
14. L. Sun *et al.*, *J. Biol. Chem.* **269**, 26449 (1994).
15. We labeled cell surface TGF-β receptors by cross-linking them to ^{125}I-labeled human TGF-β1 (*14*). Labeled receptors were resolved by SDS–polyacrylamide gel electrophoresis and visualized by autoradiography.
16. F. López-Casillas *et al.*, *Cell* **73**, 1435 (1993).
17. F. Boyd and J. Massagué, *J. Biol. Chem.* **264**, 2272 (1989); M. Laiho *et al.*, *ibid.* **266**, 9108 (1991); M. Laiho *et al.*, *ibid.* **265**, 18518 (1990).
18. RII was amplified from cDNA with the reverse transcriptase–polymerase chain reaction (RT-PCR) and was transcribed and translated in vitro essentially as described by S. Powell *et al.*, *N. Engl. J. Med.* **329**, 1982 (1993). PCR products were either directly sequenced or were cloned into the pCRII cloning vector (Invitrogen), and then the DNA sequences of pooled or individual RII clones were determined. The wild-type RII sequence we used as a reference is that updated as GenBank accession no. M85079. Primers used for amplification and sequencing are available from the authors upon request.
19. The predicted COOH-terminal sequence of the VACO481 RII mutant, beginning with Val^{534} is ValTrpGlnAsnAlaSerValSerTrpSerIleTrpThrGlySerArgGlyGlyAlaAlaArgArgArgArgPheLeuLysThrAlaPro. Sequence changes which we presume to be polymorphisms, because they were present in both the VACO481 tumor and the matched normal tissue, included a C to T change at nucleotide 1651 (converting Ala^{439} to Val), and an A to C change at nucleotide 2040 in the 3′ untranslated region.
20. K. Hagan *et al.*, *Mol. Cell. Biol.* **15**, 809 (1995).
21. N. Papadopoulos *et al.*, *Science* **263**, 1625 (1994); C. Bronner *et al.*, *Nature* **368**, 258 (1994); R. Fishel *et al.*, *Cell* **75**, 1027 (1993); F. Leach *et al.*, *ibid.*, p. 1215; N. Nicolaides *et al.*, *Nature* **371**, 75 (1994).
22. A. Avery *et al.*, *Br. J. Cancer* **68**, 137 (1993).
23. M. Brattain, G. Howell, L. Sun, J. K. V. Willson, *Curr. Opin. Oncol.* **6**, 77 (1994).
24. J. Eshleman and S. Markowitz, *ibid.* **7**, 83 (1995).

25. We thank T. Pretlow and the Westem Division of the Cooperative Human Tissue Network (CHTN) for assistance. Supported by the following grants: NIH grants CA63480 (L.-Z.S.), CA38173 and CA50457 (M.B.), CA51504 and CA57208 (S.M.), P01 CA51183 (J.K.V.W. and S.M.), CA62924, CA35494, and CA09320 (B.V., K.W.K., R.P.), and P30 CA4370301 to the Case Westem Reserve University Cancer Center; American Cancer Society grant FRA-451 (S.M.); and the Clayton Fund (B.V.). B.V. is an American Cancer Society Research Professor and an investigator of the Howard Hughes Medical Institute.

1 February 1995; accepted 5 April 1995